Glass Technol.: Eur. J. Glass Sci. Technol. A, October 2013, 54 (5), 177–184

Effects of substrate and long term corrosion on PVD-multilayer coatings for architectural glazing

Robert Meszaros,[1] *Michael Wild*[2] *& Lothar Wondraczek*[1,3,4]*

[1] *Department of Materials Science, University of Erlangen-Nuremberg, 91058 Erlangen, Germany*
[2] *Interpane Glasgesellschaft mbH, 94447 Plattling, Germany*
[3] *Otto-Schott-Institute, University of Jena, 07743 Jena, Germany*
[4] *Energie Campus Nürnberg, 90403 Nuremberg, Germany*

Manuscript received 26 February 2013
Revision received 6 May 2013
Manuscript accepted 6 May 2013

We report on the effects of substrate quality and long term environmental exposure on the performance of PVD-coated soda–lime–silica glasses for architectural glazing. Coated and uncoated glasses were stored in conditions simulating commercial packing at relative humidities of 5, 45 and 95% for a period of up to 64 weeks, and analysed for surface alterations. The effect of specific stages of substrate corrosion on coating performance was evaluated by applying coatings on pre-corroded samples. Subsequent thermal treatment of as-coated, pre-corroded samples was considered in order to account for the effect of thermal post-processing. The corrosion state of the incoming substrate material is shown to significantly affect the later coating procedure and performance. Critical storage requisites are derived to ensure effective coating deposition.

1. Introduction

Functional multilayer coatings such as low emissivity (low-E) and solar control coatings for architectural or automotive applications are commonly deposited on soda–lime–silica (SLS) float glass.[1–3] SLS float glass is generally an excellent substrate material for large area coatings due to its inherent high surface quality, low cost and ready availability. However, in the presence of humidity, atmospheric gases and temperature fluctuations during production, transport, storage and/or subsequent processing, the surface of the glass undergoes complex chemical and topological changes, known as glass surface corrosion or weathering. *Glass corrosion*, typically referring to the interaction between glasses and liquids, is extensively described in literature. On the other hand, *weathering*, the interaction with gases and humidity is still a matter of many unknowns.[4–7] Current interpretations particularly describe condensation-induced dealkalisation and the formation of a hydrated layer (gel layer) on the glass surface. Subsequent reactions with gaseous atmospheric constituents lead to the precipitation of hydrate, carbonate and hydrocarbonate crystalline products of silicon, calcium and sodium. Advanced stages of weathering usually result in hazy white layers, whereas in the early stages, the effects are almost invisible, but may still result in significant changes in physical properties.[8–13]

For the application of optical quality thin films with a thickness of less than 100 nm, a pristine, defect-free glass surface is crucial. Glass alteration and its reaction products, as described above, often lead to optical changes, loss of function and reduced chemical and mechanical reliability of such coatings.[14] This is particularly the case when the coatings are applied *off-line*, i.e. when glass production and coating application occur in separated processes, or when a subsequent thermal or other post-treatment of the coated glass is required such as with thermal toughening or bending.[2,15] If coatings are applied on such *pre-corroded* glass surfaces, they may be affected in many ways. For example, the migration of sodium from the glass into the coating may cause crystallisation or other phase changes, which can strongly affect the optical appearance, adhesion and, hence, functionality of the coating.[16] To overcome this problem, sodium-blocking layers (e.g. amorphous refractory materials with low sodium diffusivity such as SiO_2, TiO_2, Al_2O_3 or Si_3N_4 have been introduced.[17,18] Such layers function well when coatings are applied onto pristine glass where films can grow without structural defects. In the case of a corroded glass surface, nanoscopic to microscopic crystallites and, more generally, surface property gradients may lead to pinholes, cracks and grain boundaries which form in the coating during deposition. This may result in reduced activation energies for diffusion processes, particularly during thermal post-processing.

In this study, we systematically investigate the effect of weathering on the surface of SLS float glass and subsequent PVD coating and tempering steps. From the obtained data, we deduce recommendations for glass storage.

*Corresponding author. Email lothar.wondraczek@uni-jena.de

2 Materials and methods

2.1. Sample preparation

Experiments were performed on as-received commercial float glass (f-glass GmbH, Sülzetal, Germany) with a thickness of 3·8±0·05 mm. A large glass sheet was taken from a single melt campaign without application of any protective coating, to ensure samples had identical surface properties and were the same age. For storage and coating experiments, glass plates of 20×20 cm^2 size were prepared by using an automatic glass cutting machine. Substrate glasses and coated glasses were washed in an industrial washing machine with deionized water and rotating polyamide brushes. As a model coating, a commercial temperable low emissivity (low-E) multilayer coating was deposited in an industrial magnetron sputtering line (Interpane Glasgesellschaft mbH, Plattling, Germany). The coating consists of stacked layers of MeO_x/NiCr/Ag/NiCr/MeO_x, with MeO_x=[SiO_2, ZnO, TiO_2, SnO] with a total thickness of 100±2 nm.[19]

2.2. Storage experiments

Storage experiments were performed on packages of as-received and low-E coated coated glasses, each stack containing 20 plates separated by ~120 mg/m^2 polymethyl methacrylate (PMMA) spacer beads with a mean diameter of 120±15 μm (AC Separol G, Aachener Chemische Werke, Mönchengladbach, Germany). The package was clamped between two resin bonded paper composite plates (Ullmann Plastic GmbH, Germany) and tightened with four screws at 1 N m torque to simulate commercial storage and packaging conditions. The packages were then stored at 21±2°C and constant relative humidity (r.h.) of 5, 45 and 95±3%. 5 and 95% r.h. were generated in 40×30×30 cm^3 sealed polypropylene boxes, using silica gel for the dry and 1·5 l oversaturated potassium nitrate solution for the humid atmospheres, respectively. Storage at 45% r.h. was obtained in a climate controlled room. The aforementioned sealed polypropylene boxes were stored in the same room to provide an identical temperature. The relative humidity was checked weekly by hygrometers mounted inside the boxes. Samples were taken for examination after two, four, eight, 16, 32 and 64 weeks of storage. Coated glass samples were cleaned from the spacer beads with an argon gun and cut into 2×4 cm^2 representative pieces of from the centre of the glass plates. Half of the uncoated, as-corroded glass plates were rinsed in double distilled water, dried in an argon jet to remove the spacer beads as well as loose and water soluble degradation products, and finally cut. The remaining as-corroded glass plates were washed in a commercial flat glass washing machine and post-coated with the previously described low-E coating. All samples were stored in a dry desiccator until further analysis.

2.3. Analytical methods

Topographical effects of glass surface corrosion were analysed by optical microscopy (OM, Olympus BX50, Hamburg, Germany) equipped with a digital camera (Olympus XC50, Hamburg, Germany), by environmental scanning electron microscopy (ESEM, Quanta 200, FEI, Prague, Czech Republic) equipped with energy dispersive x-ray analysis (EDX) and by atomic force microscopy (AFM, Veeco Dimension 3100, Veeco Instruments, NY, United States) in contact mode under ambient conditions, using a silicon tip with a nominal tip radius of 6 nm (NT-MDT, NSG10/50). AFM scans were recorded at different sample locations over areas of 20×20 μm^2 and 100×100 μm^2 in size. Images were processed using the Gwyddion 2·22 software package.

Corrosion induced changes in optical properties were examined by ultraviolet-near infrared (UV-NIR) spectroscopy (Lambda 950, Perkin Elmer, Unterhaching, Germany) and Fourier-transform infrared spectroscopy (FTIR, Nicolet Impact 420, Thermo, Dreieich, Germany). Ultraviolet-NIR spectra were recorded over a range of 200–2500 nm and FTIR spectra over a range of 2500–18000 nm, using a resolution of 5 nm. The impact of corrosion on the efficiency of the low-E coating was determined for a wavelength of 2 μm using

$$\tau_{(2\,\mu m)} = \frac{T_x - T_s}{T_0 - T_s} \quad (1)$$

where T_x is the transmission of the as-corroded coated glass, T_s the transmission of uncoated pristine glass and T_0 the transmission of coated pristine glass. The colour of the coatings was determined in the CIE1976

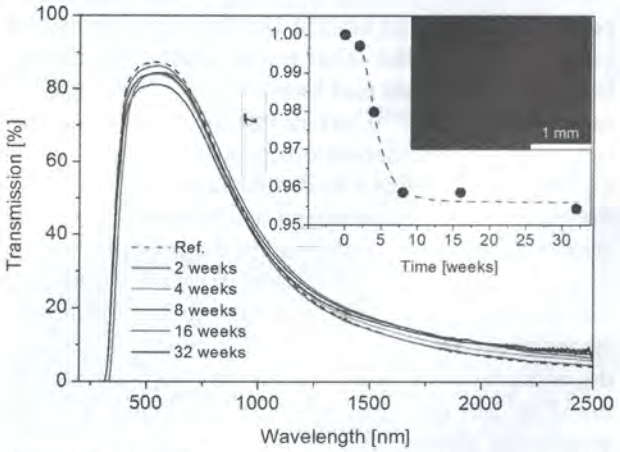

Figure 1. Evolution of ultraviolet-NIR transmission of low-E coated SLS float glass during storage for 64 weeks at 95% r.h. The insets show the respective coating efficiency and a microscopic image of the humidity induced defects developing in the coating [Colour available online]

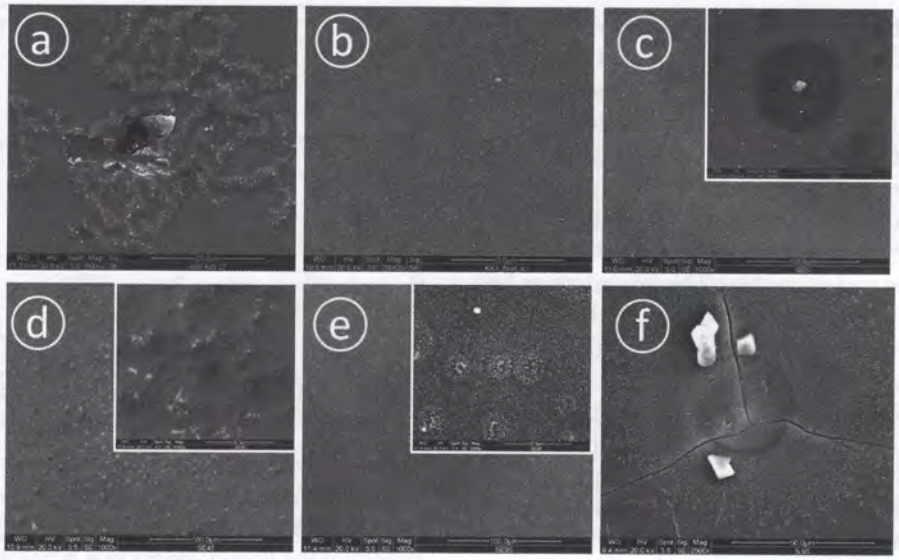

Figure 2. SEM micrographs of (A) low-E coated (B) fresh and the air side of as-corroded SLS float glass after 64 weeks at (C) 5% r.h. (D) 45% r.h. and (E and F) 95% r.h. The insets present respective micrographs at higher magnification

L*a*b colour space from reflectance spectra collected over a range of 340–830 nm for a 10° observer at D65 constant luminosity according to ISO 11664. For colour visualisation the L*a*b values were transferred into the CIE XYZ colour space.

The molecular structure and the relative extent of glass surface leaching was analysed by attenuated reflection FTIR spectroscopy (ATR-FTIR), with the glass surface facing a ~7 mm^2 analytical area on a ZnSe crystal. For each sample, a set of 64 reflectance spectra was collected at a resolution of 4 cm^{-1}.

Mechanical properties were studied using the DIN EN ISO 1288-5 ring-on-ring biaxial flexural strength test and dynamic nanoindentation in accordance with a previous study.[20] Previously reported data is used here for illustration and extended with additional data points for long term storage (64 weeks). For these new data points, each test series was conducted on 12 quadratic specimens with edge length l=60±0·8 mm and otherwise identical test parameters to the previous data[20]. Similarly, dynamic nanoindentation measurements were adopted from this previous study and completed with further data points for the long term exposure.[20]

3. Results and discussion

3.1. Corrosion of as-coated glass

Optical and SEM micrographs of the surface of samples stored at low and intermediate humidity (5 and 45% r.h.) show no remarkable signs of corrosion within the whole time of storage. For high humidity (95% r.h.), point defects initially ~5–20 μm size were observed within the first two weeks of storage (inset, Figure 1). Corresponding transmission spectra of the corroded coatings show continuously decreasing NIR-transmission and an irregular change of Vis-transmission with increasing storage time (Figure 1). The efficiency as a measure of the low-E performance shows a ~5 % decrease within 8 weeks of corrosion, but remains at a constant value for further storage (inset, Figure 1). SEM micrographs (Figure 2(a)) and AFM profiling of the defects after removal of the loose residues using a soft tissue indicate delamination of the coating at a depth of 50±2 nm, which is the position of the silver layer. The delamination effect is assumed to result from humidity-activated restructuring and agglomeration of the silver component of the coating, where at small pin-holes, water diffuses into the coating and triggers the release of internal stresses, which in turn lead to the point-like wrinkling pattern of the top layers.[21] To compare the effect of weathering on coated and uncoated glass, the biaxial flexural strength was determined previously as a measure of the size of surface defects.[20,22]

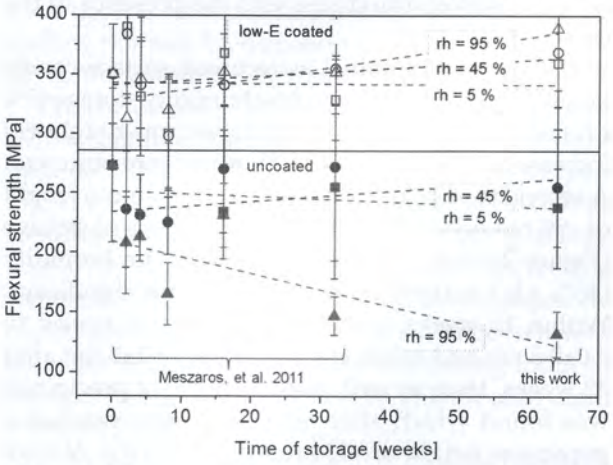

Figure 3. Ring on ring biaxial flexural strength evolution of the air-side of SLS float glass with and without low-E coating during 64 weeks of storage at 5, 45, 95% r.h. Lines are guides for the eye [Colour available online]

Figure 3 shows the development of the biaxial flexural strength depending on storage time and humidity for the low-E coated and the uncoated, as-corroded float glass air side. As a result of weathering and, hence, growth of surface defects, the flexural strength continuously decreases in case of the high humidity storage (95% r.h.). On the other hand, coated glasses do not lose their flexural strength within the considered storage time and humidity. This observation has been related to a protective function of the coating which prevents water from interacting with the glass surface.[20]

As a conclusion, it appears that corrosion of an as-coated glass specimen which was not previously exposed to weathering (before coating application) occurs only in the coating itself. Even for high humidity, no significant, surface related corrosion effect could be observed after 64 weeks of exposure. As long as the PVD coating remains intact, it is practically impermeable to water molecules.

3.2. Glass surface corrosion

In order to examine the effect of pre-corrosion on coating deposition and performance, to-be-coated glass samples were weathered in a defined way. Since coatings were deposited only on the air side of the glass, tin-side corrosion will not be considered in the following. A first indicator for humidity-induced surface alteration is an increase in surface roughness[23] and relevant data are shown in Figure 4. The as-received float glass had an initial root mean square (rms)-roughness of 1·1±0·1 nm (determined over an area of 1×1 μm^2), with occasional features ranging up to ~ 58 nm and regularly distributed over the whole surface, also confirmed by SEM analysis (Figure 2(b)). The latter are calcium sulphate crystallites which result from glass production.[24] Rinsing and blowing with argon had no significant influence on the observed roughness and the presence of the crystallites.

Comparing the initial as-received surface condition with glass corroded in low humidity storage (5% r.h.) only marginal surface changes (rms roughness increase to 3·0±0·8 nm over 64 weeks) were observed. A second type of precipitate with a maximum height of ~90 nm occurred within the last weeks of storage (Figure 2(c)). In contrast, at intermediate humidity (45% r.h.) surface changes were more significant. Within 16 weeks, the rms roughness increased to 5·0±0·8 nm and reached a plateau at 11·1±3 nm after 32 weeks. Here as well, a second type of precipitate was found which after 64 h of storage reached a maximum height of ~134 nm (Figure 2(d)). At high humidity (95% r.h.) drastic roughness and morphological changes were observed from the beginning of storage. A rms roughness of 11·3±1·0 nm and precipitates larger than 300 nm in height were observed

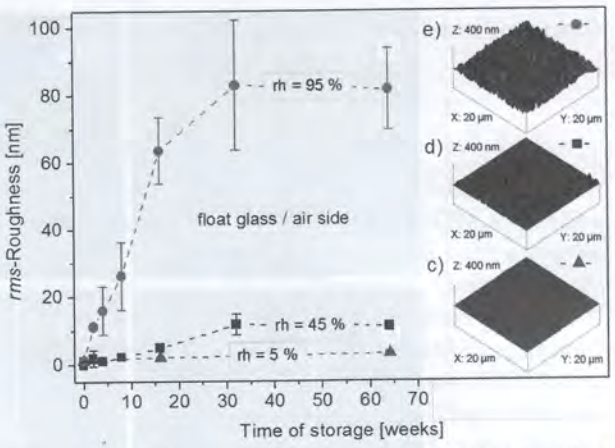

Figure 4. Development of rms-roughness of the air side of SLS float glass during storage at 5, 45 and 95% r.h. and 21°C up to 64 weeks. Inset: AFM topological surface scan images of the float glass air side surface after 64 weeks of storage at respective humidity. Lines are guides for the eye [Colour available online]

already after 2 weeks of storage. After 32 weeks, the rms roughness increased to 80±20 nm with individual features larger than 2·2 µm. The insets in Figure 4 show the final AFM topography of the glass surfaces at (a) high, (b) intermediate, and (c) low humidity after 64 weeks of exposure. The largest defects (~50 µm in height) were found in the contact area and in the surrounding area between the spacer beads and the glass. The spacer beads seem to penetrate into the gel-layer, producing a calotte-like impression surrounded by a variety of precipitates of different size (Figure 2(f)). It is assumed that due to capillary effects, humidity preferentially condensates in the glass/bead contact area. This in combination with mechanical pressure locally enhances leaching of glass constituents. At elevated humidity, the first traces of such spacer bead impressions can already be found

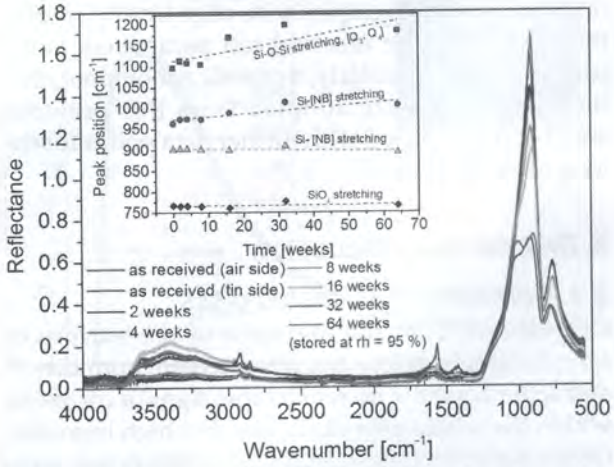

Figure 5. Evolution of FTIR-ATR spectra for the surface of SLS float glass during storage for 64 weeks at 95% r.h. The insets show the shift in peak position of the main SiO_2, [Q_x] and SiO-[NB] peaks [Colour available online]

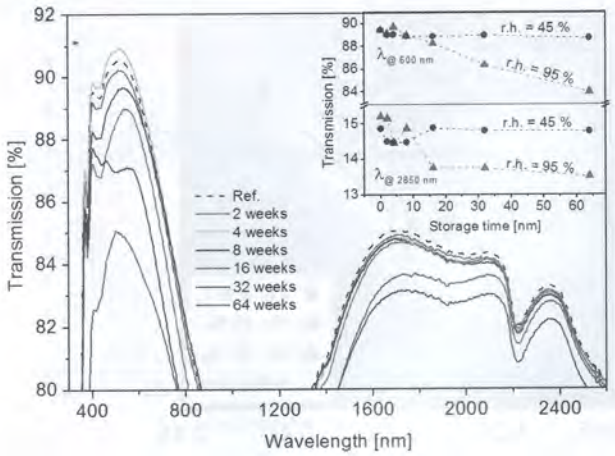

Figure 6. Evolution of ultraviolet-NIR transmission of SLS float glass during storage for 64 weeks at 95% r.h. The inset shows the respective development in VIS (λ=600 nm) and NIR transmission (λ=2850 nm) compared to float glass stored at 45% r.h. [Colour available online]

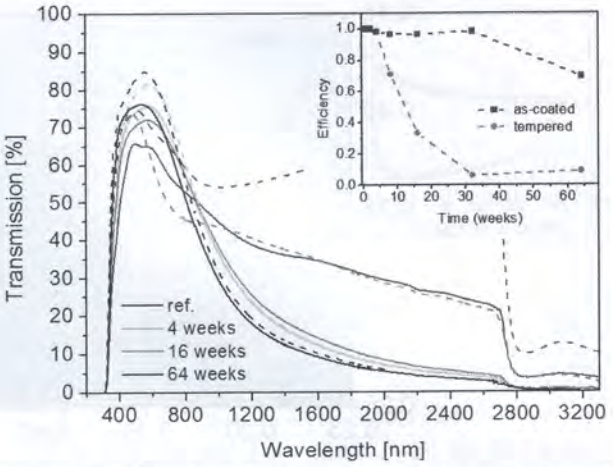

Figure 7. Evolution of ultraviolet-NIR transmission of as-coated, pre-corroded float glass during storage for 64 weeks at 95% r.h. before (full lines) and after (dashed lines) tempering at 700°C for 3 min. The inset compares the respective IR-efficiency evolution between the untempered and a tempered coating stored at 95% r.h. [Colour available online]

after 4 weeks of storage. EDX spectra of sufficiently large precipitates indicate silicon-free carbon carbonates of calcium with additional secondary amounts of sodium and magnesium.

The formation of a gel layer at the glass surface was observed by ATR-FTIR spectroscopy; example spectra are shown in Figure 5. The inset of Figure 5 shows the change of band position with increasing weathering time (based on Gaussian fitting of the SiO_4, Si–OH and Si–O–[NB], [Q_x] bands).[25] The Si–O–Si and the Si–OH peaks shift to higher wavenumbers with increasing exposure time. Also, a broad OH-related band develops in the range between 3600–3000 cm^{-1}, which can be attributed, in combination with the small sharp peaks at 2900 and 1500 cm^{-1}, to hydrated carbonates of sodium, calcium and silicon, e.g. trona, gaylussite or pecolite.[26] The hydration of the glass surface is further confirmed by FTIR transmission spectra showing an intensity increase in the water absorption peak at 2850 nm (inset of Figure 6).

The impact of corrosion on the optical properties of the coating is shown in Figure 6. Over 64 weeks of high humidity exposure, the ultraviolet-NIR transmission decreases by ~2–5%. For samples stored at low and intermediate humidity, no corrosion effects on UV-Vis transmission could be detected, regardless of the significant increase in surface roughness.

3.3. Coating and tempering of pre-corroded glass

The quality of low-E coatings is determined by their infrared reflectance and their lateral homogeneity. Even small deviations in film thickness or single defects are readily visible to the human eye. Pre-corrosion of the substrate glass may strongly decrease the quality of a subsequently applied coating. To quantify this problem, the effect of pre-corrosion of the substrate on the properties of the coating was examined. Transmission spectra of as-coated, high humidity pre-corroded glasses before and after tempering are shown in Figure 7. Between the as-coated and the tempered states, a non-uniform increase in visible transmission of ~10% is found. The colour of the coating changes from bluish before tempering to approximately neutral to greenish after tempering (Figure 8). This colour change is attributed to the partial oxidation of the NiCr component in the coating.[27] The surface topography of the coatings is shown in Figure 9. After tempering, regularly distributed white dots with a diameter of ~1 μm are found. These are identified as agglomerates of metallic Ag. The agglomeration effect of the thin silver film is a well-known problem of thermally annealed low-E coatings. It is related to size-induced reduction of the melting point of Ag, diffusion and (de-)wetting of the silver film within the surrounding coating layers.[28–30]

Pre-corrosion of the glass substrate is associated with a continuous decrease in coating efficiency τ of up to 60 % (Figure 7), especially after further tempering. This effect commences within the first two weeks of substrate weathering. For pre-weathering at high humidity, a transmission increase with increasing weathering time can be observed on the subsequently coated glass over the whole infrared range (whereas the glass itself does not exhibit weathering-induced changes in infrared transmission at least after eight weeks of storage, Figure 6).

Pre-weathering at low and intermediate humidity (5% and 45% r.h.) did not result in significant changes in the efficiency of the as-coated low-E glass. However, also for these mild storage conditions, optical and scanning electron microscopy reveal defects

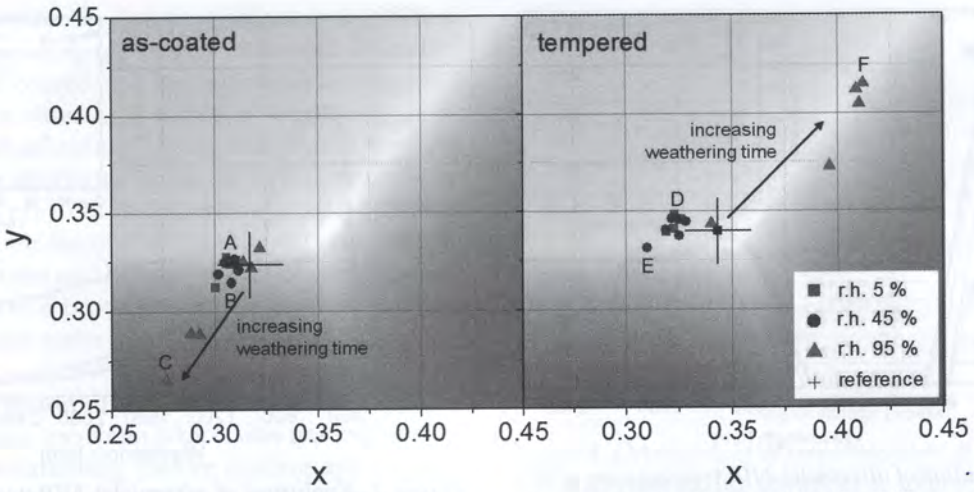

Figure 8. Colour deviation determined from VIS-reflectance measurements displayed in the CIE xy colour space at constant luminosity for as-coated, pre-corroded SLS float glass during storage for 64 weeks at 5, 45 and 95% r.h. before (as-coated) and after tempering [Colour available online]

and changes in the appearance of the coatings, as is exemplarily shown in Figure 9(A–B) for 64 weeks of pre-weathering.

The effect of pre-weathering can also be seen in the colour change of as-coated and tempered samples (Figure 8). Generally, as-coated samples develop an increasingly bluish tint with increasing time of pre-weathering. The effect is significantly more pronounced for high humidity weathering. It is worth noting that the initial (first 1–8 weeks) colour deviation from the reference might be also due to ageing effects of the coating, since it is known that PVD coatings tend to undergo structural changes during the first weeks after deposition.[14] As already noted, subsequent tempering of the samples which were pre-weathered at high humidity lead to a strong colour shift (Figure 8). Micrographs of the tempered coatings on pre-corroded glass show a variety of severe defects deriving from the corroded glass surface (Figure 9(f)). These defects enable oxidation of the silver component during tempering and, hence, yellowish coloration. The effect is much less pronounced for low or intermediate humidity storage.

The variation of surface mechanical properties with progressing corrosion is shown in Figures 10–11. For the uncoated samples, this is in good agreement with a recent report by Gonzalez Rodriguez & Hand.[31] We consider that data from the first 20–40 nm of the surface layer should be neglected because in this regime, indentation data are strongly affected by tip geometry and other experimental conditions. For weathering at low and intermediate humidity, higher hardness is generally found for the low-E coated glass as compared to the uncoated SLS. The Young's modulus of the coatings is ~85 GPa, compared to a value of ~70 GPa for the uncoated glass. The hardness

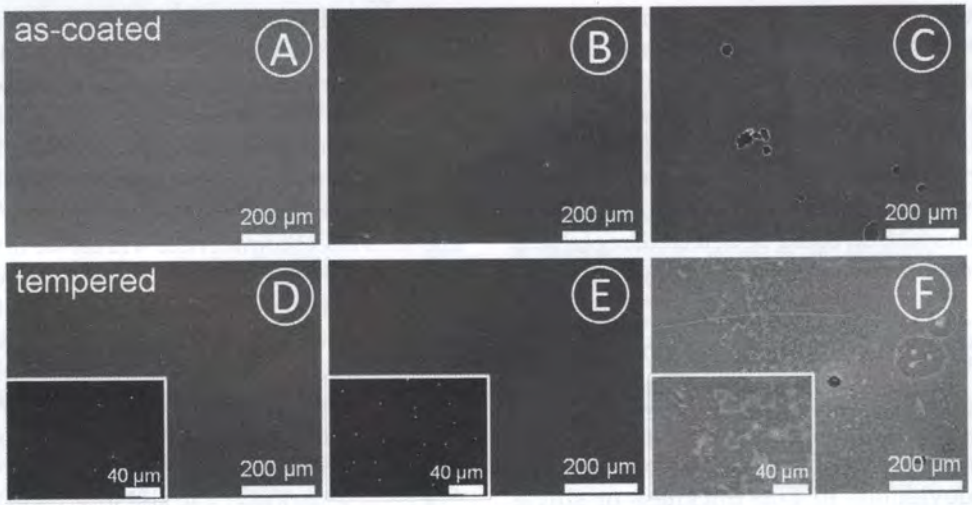

Figure 9. Optical micrographs of as-coated, pre-corroded SLS float glass after substrate glass storage for 64 weeks at (A) 5% r.h. before tempering, (B) 45% r.h. before tempering and (C) 95% r.h. before tempering, (D) 5% r.h. after tempering, (E) 45% r.h. after tempering and (F) 95% r.h. after tempering. The insets present respective micrographs at higher magnification [Colour available online]

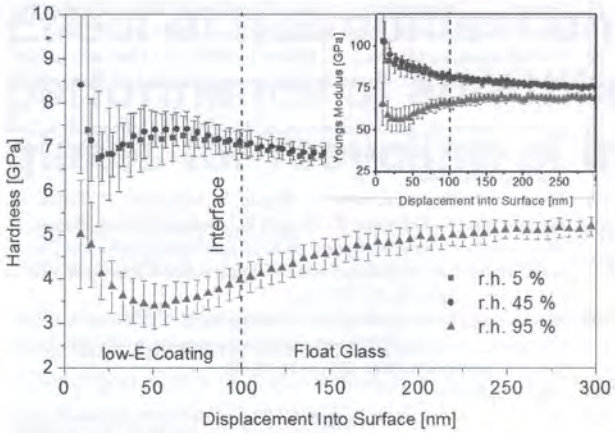

Figure 10. Effective hardness and Young's modulus (inset) as a function of indentation depth for low-E as-coated, pre-corroded SLS float glass after storage for 8 weeks at 5, 45 and 95% r.h. as obtained by Berkovich nanoindentation [Colour available online]

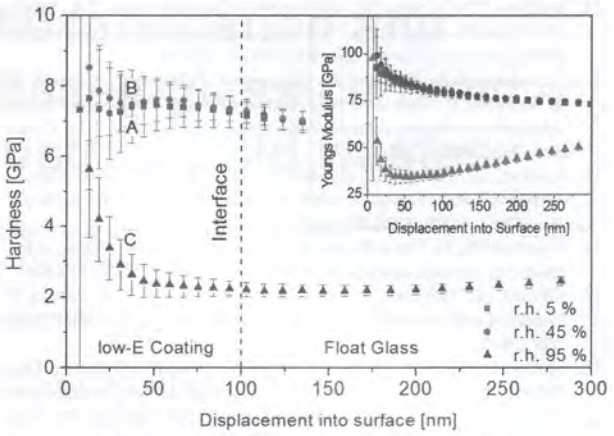

Figure 11. Effective hardness and Young's modulus (inset) as a function of indentation depth for low-E as-coated, pre-corroded SLS float glass after storage for 32 weeks at 5, 45 and 95% r.h. as obtained by Berkovich nanoindentation [Colour available online]

of the coated specimen converges to 6·5 GPa when an indentation depth of 200 nm is exceeded, i.e. the value of the uncoated glass. Indentation of the coatings on pre-corroded glass show strongly decreased hardness and modulus values with increasing storage time. After 8 weeks of storage, the coatings exhibited an apparent elastic modulus of ~55 GPa and a hardness ~3·5 GPa, again converging to the hardness of the float glass when the indentation depth exceeded 350 nm (Figure 9). After weathering for 32 weeks, this effect is even more pronounced. Neglecting the influence of the coating, the experiments reveal the mechanical properties of the growing gel layer on the air side of float glass, which is mechanically weaker than the bulk glass and covers more than 400 nm of the surface layer. For the freshly coated glass, the protective function of coating is confirmed. If the coating is applied on a pre-corroded glass, not only the initial coating performance, but also its long-term properties during progressing weathering are negatively affected.

4. Conclusions

The impact of weathering, substrate corrosion and subsequent thermal processing on the performance of low-E PVD multilayer coatings was investigated systematically over a time of 64 weeks under various storage conditions. Results confirmed the protective function of the low-E coating when applied on pristine glass substrates. When exposed to high humidity, delamination occurs in the coating stack itself, resulting in decreasing efficiency and visual changes in the colour of the coating. After long term weathering, delamination and coating damage may progress until the protective function is lost. Application of the coating on pre-weathered substrates, on the other side, is strongly dependent on storage conditions. Float glass stored for more than two to four weeks at high humidity could not be coated in an efficient way. Storage at intermediate and low humidity was acceptable to up to 16 weeks. However, continuous variations in colour towards a bluish tint were observed also for mild substrate storage. Surface chemical and mechanical analysis revealed the formation of an alkali-depleted gel layer at the glass/coating interface with strongly decreased hardness and Young´s modulus, ranging more than 300 nm into the glass surface.

Acknowledgement

The authors gratefully acknowledge financial support from the Bayerische Forschungsstiftung through the program FORGLAS - Glasses for energy efficient building technologies.

References

1. Greenberg, C. B. Thin films on float glass: the extraordinary possibilities. *Ind. Eng. Chem. Res.*, 2000, **40** (1), 26–32.
2. Finley, J. J. Heat treatment and bending of low-E glass. *Thin Solid Films*, 1999, **351** (1–2), 264–73.
3. Arbab, M. & Finley, J. J. Glass in architecture. *Int. J. Appl. Glass Sci.*, 2010, **1** (1), 118–29.
4. Scholze, H. Glass-water interactions. *J. Non-Cryst. Solids*, 1988, **102** (1–3), 1–10.
5. Hench, L. L. & Clark, D. E. Physical chemistry of glass surfaces. *J. Non-Cryst. Solids*, 1978, **28** (1), 83–105.
6. Baucke, F. G. K. Corrosion of glasses and its significance for glass coating. *Electrochim. Acta*, 1994, **39** (8–9), 1223–8.
7. Stockdale, G. F. & Tooley, F. V. Effect of humid conditions on glass surfaces studied by photographic and transmission techniques. *J. Am. Ceram. Soc.*, 1950, **33** (1), 11–16.
8. Feldmann, M. & Weißmann, R. Initial stages of float glass corrosion. *J. Non-Cryst. Solids*, 1997, **218**, 205–9.
9. Schmitz, I., Schreiner, M., Friedbacher, G. & Grasserbrauer, M. Tapping-mode AFM in comparison to contact-mode AFM as a tool for in situ investigations of surface reactions with reference to glass corrosion. *Anal. Chem.*, 1997, **69** (6), 1012–18.
10. Hayashi, Y., Fukuda, Y. & Kudo, M. Investigation on changes in surface composition of float glass - mechanisms and effects on the mechanical properties. *Surf. Sci.*, 2002, **507–510**, 872–6.